The Journal of Experimental Biology 205, 1471–1484 (2002)
Printed in Great Britain © The Company of Biologists Limited 2002
JEB4046

Brainstem lateral line responses to sinusoidal wave stimuli in still and running water

Sophia Kröther*, Joachim Mogdans and Horst Bleckmann
Institut für Zoologie, Universität Bonn, Poppelsdorfer Schloß, D-53115 Bonn, Germany
*Author for correspondence (e-mail: kroether@uni-bonn.de)

Accepted 11 March 2002

Summary

The fish lateral line consists of superficial and canal neuromasts. In still water, afferent fibers from both types of neuromast respond equally well to a sinusoidally vibrating sphere. In running water, responses to a vibrating sphere of fibers innervating superficial neuromasts are masked. In contrast, responses of fibers innervating canal neuromasts are barely altered. It is not known whether this functional subdivision of the peripheral lateral line is maintained in the brain. We studied the effect of running water on the responses to a 50 Hz vibrating sphere of single units in the medial octavolateralis nucleus (MON) in goldfish *Carassius auratus*. The MON is the first site of central processing of lateral line information. Three types of units were distinguished. Type I units (*N*=27) were flow-sensitive; their ongoing discharge rates either increased or decreased in running water, and as a consequence, responses of these units to the vibrating sphere were masked in running water. Type II units (*N*=7) were not flow-sensitive; their ongoing discharge rates were comparable in still and running water, so their responses to the vibrating sphere were not masked in running water. Type III units (*N*=7) were also not flow-sensitive, but their responses to the vibrating sphere were nevertheless masked in running water. Although interactions between the superficial and canal neuromast system cannot be ruled out, our data indicate that the functional subdivision of the lateral line periphery is maintained to a large degree at the level of the medial octavolateralis nucleus.

Key words: lateral line, medial octavolateralis nucleus, neuromast, hydrodynamic stimuli, background noise, goldfish, *Carassius auratus*.

Introduction

Fishes use the lateral line to detect miniscule water motions (for reviews, see Bleckmann, 1994; Coombs and Montgomery, 1999). The behavioral relevance of the lateral line has been documented in studies on prey capture (e.g. Hoekstra and Janssen, 1985; Montgomery and Hamilton, 1997; Montgomery and Coombs, 1998), predator avoidance (e.g. Blaxter and Fuiman, 1989), schooling (e.g. Partridge and Pitcher, 1980; Pitcher, 1979; Pitcher et al., 1976), mating (e.g. Matsushima et al., 1989; Satou et al., 1991a,b), obstacle avoidance (e.g. von Campenhausen et al., 1981; Hassan, 1989; Weissert and von Campenhausen, 1981) and rheotaxis (Baker and Montgomery, 1999; Montgomery et al., 1997).

The sensory organs of the lateral line are the neuromasts, which can be distributed across the entire fish body (Northcutt, 1989). Each neuromast consists of a patch of hair cells underneath a gelatinous cupula. Two types of neuromast can be distinguished: superficial neuromasts (SN), which occur freestanding on the surface of the skin, and canal neuromasts (CN), which are recessed in subepidermal canals (e.g. Münz, 1979; Webb, 1989; Song and Northcutt, 1991).

Neuromast function has been studied in a still-water environment in various ways: by direct observation of cupula motion (Denton and Gray, 1988, 1989), or by recording from lateral line hair cells (e.g. Harris et al., 1970), or by recording neural activity of primary afferent fibers in response to the water motions caused by a stationary vibrating sphere, i.e. a dipole stimulus (e.g. Münz, 1985; Kroese and Schellart, 1992; Coombs and Janssen, 1990; Coombs and Montgomery, 1992; Montgomery and Coombs, 1992; Wubbels, 1992; Montgomery et al., 1994). The latter studies revealed that the response of the fibers innervating superficial neuromasts is approximately proportional to the relative velocity of the fish and the surrounding water; thus superficial neuromasts function as velocity detectors. Lowest displacement thresholds are in the frequency range 20–60 Hz. In contrast, the response of fibers innervating canal neuromasts is largely proportional to net water acceleration; thus canal neuromasts function as acceleration detectors. In addition, canal neuromasts function as high-pass filters and have minimal displacement thresholds in the frequency range 60–120 Hz.

Afferent fibers that innervate superficial and canal neuromasts exhibit different sensitivity to running water (Engelmann et al., 2000; Voigt et al., 2000). Fibers innervating superficial neuromasts are flow-sensitive, with increased

ongoing discharge rates in running water. In contrast, fibers innervating canal neuromasts are flow-insensitive, i.e. with comparable ongoing discharge rates in still and running water.

Engelmann et al. (2000) were the first to record the responses of primary lateral line afferent fibers to a stationary vibrating sphere in running water. They found in goldfish that fibers innervating superficial neuromasts respond highly sensitively to a vibrating sphere only in still water. In running water responses were masked, because superficial neuromasts were permanently stimulated by the background water flow. Responses of fibers innervating canal neuromasts to the vibrating sphere were barely affected by running water, indicating that canal neuromasts act as high-pass filters. Thus, in addition to the morphological separation, there is a clear functional separation of the peripheral lateral line.

The sensory information that is represented by the activity of primary afferent fibers is processed by neurons in the medial octavolateralis nucleus (MON) in the fish brainstem (Puzdrowski, 1989; New et al., 1996). Studies using vibrating sphere stimuli have shown that many MON units exhibit primary-like responses and receptive fields; the latter may be explained by the processing of peripheral input through a lateral inhibitory network (Coombs et al., 1998). Receptive fields that are completely unlike those of primary afferents can also be found among MON units (Mogdans and Kröther, 2001). Studies in which the lateral line was stimulated with water motions generated by a moving object indicate that MON neurons integrate information from many neuromasts, which may be distributed across large portions of the lateral line periphery (Mogdans et al., 1999; Mogdans and Goenechea, 2000). Thus, there are at least two channels in the lateral line brainstem, one to process local hydrodynamic information generated, for example, by a vibrating source, and another to process more complex water motions such as those generated by a moving source (Mogdans and Goenechea, 2000). However, the extent to which the functional separation of the lateral line periphery (Engelmann et al., 2000) is maintained in the brainstem is unknown. To answer this question, we studied how the responses of goldfish MON units to a stationary vibrating sphere are affected by running water.

Materials and methods

Animal handling

Experiments were conducted with 14 goldfish, *Carassius auratus* L., ranging from 5.4 cm to 9.2 cm in standard body length. Animals were obtained from commercial suppliers and housed in groups of 30 fish in 250 l tanks maintained at 20–23 °C. Fish were deeply anesthetized with ice-cold water, immobilized by intramuscular injection of 10–20 µl pancuronium bromide (Organon Teknika) and respirated with water flowing through a silicone tube into the mouth. In addition, Xylocaine (2 %, Astra Chemicals) was applied to the top of the skull before careful removal of the skin at the preparation site with the blade of a surgical knife. A small hole was drilled into the skull using a dental drill, exposing the left (ipsilateral) side of the brain, between the caudal part of the cerebellum and the rostral part of the vagal lobe. Fatty tissue covering the brain was aspirated and the brain was kept moist with a physiological salt solution (Oakley and Schafer, 1978). To prevent water from penetrating the brain, a plastic cylinder was glued onto the top of the skull. After surgery the fish were transferred to a flow tank (dimensions 90 cm×60 cm, canal width 15 cm, canal height 13 cm) and positioned in a stainless steel fish-holder, which consisted of a mouthpiece for artificial respiration with fresh water (flow rate 50–70 ml s^{-1}) and two screws by which the head was kept in a fixed and stable position. The fish were submerged 1 cm below the water surface and both sides of the fish were exposed to the open water in the flow tank.

Stimulation

Sinusoidal water motions were generated by a stationary vibrating sphere (8 mm diameter). The sphere was attached to a minishaker (LDS V101) by a stainless steel rod (2 mm diameter, 17 cm length). The shaker was driven using a 50 Hz signal (duration 1 s, rise/fall time 100 ms) generated by a computer (Power Macintosh) and read through a 14-bit D/A converter at a rate of 8 kHz (Instrunet 100B, GWI). Signals were power-amplified (LDS PA25e) and attenuated (custom-built attenuator) before being passed to the minishaker. The minishaker was mounted to a sliding bar assembly outside the tank, which allowed adjustment of sphere elevation and location along the side of the fish. The axis of sphere vibration was parallel to the long axis of the fish. The distance between the sphere and the fish was 6–7 mm. For calibration, sphere vibration in water was filmed using a video camera (see Mogdans and Kröther, 2001). Peak-to-peak (p–p) displacements at the skin of the fish were calculated using the equation given by Harris and van Bergeijk (1962). According to this equation, a sphere displacement of 100 µm, for example, resulted in a water displacement of 8.8 µm at the surface of the fish.

Water flow was generated using a model ship's propeller (8 cm diameter driven by a d.c. motor (Conrad Electronics) connected to a power supply (Voltcraft Digi 35, Conrad Electronics). The ship's propeller was suspended from a holder and moved the water on the side of the flow tank that was opposite to the side containing the fish. The water was passed through a flow collimator (15 cm×13 cm row of straws, 5 mm diameter, 15 mm length) before reaching the fish. Water velocities were calibrated without the fish in the experimental tank using particle image velocimetry (see Hanke et al., 2000). Water velocities generated at the site of the fish ranged from 1.7 cm s^{-1} to 19.4 cm s^{-1}.

Data acquisition

Neural activity from single units in the MON was recorded with glass micropipettes filled with an indium alloy (Small Parts Inc.) and plated with platinum chloride (1–4 µm tip diameter, 2–4 MΩ impedance). Electrodes were advanced through the plastic cylinder that was mounted on top of the

animal's head and placed on the surface of the brainstem with a micromanipulator. Electrodes were advanced through brain tissue in small (2–10 μm) steps using a motorized microdrive (Nanostepper NPC, Science Products Trading). Recorded activity was amplified (DAM 80, WPI), filtered (0.30–1 kHz), fed through a noise eliminator (Hum Bug, Quest Scientific), and passed through a window discriminator (WPI 121), which generated a 5 V pulse for each action potential above a selected level. Pulses were digitized (Instrunet Model 100B, 14-bit resolution, 8 kHz sampling rate), monitored and stored on a Power Macintosh using data acquisition software (SuperScope II, GWI). Original recordings were stored on a digital tape recorder (ZA5ES, Sony in combination with DTR 1802, Biologic).

Stimulation protocol

To search for lateral line units, the sphere was vibrated with a constant p–p displacement of 2700 μm and positioned at various locations along the side of the fish. A water flow velocity of 15.5 cm s^{-1} was also used. In addition, units were searched by moving the minishaker and thus the attached sphere manually along the side of the fish. If a unit responded to any of these stimuli, we tested whether it responded to airborne sound (clapping hands, shouting) or to vibrations generated by tapping against the tank walls. Units that responded to sound or vibration were assumed to receive input from the inner ear and were not investigated further.

Units that responded to the moving sphere and/or to running water but not to the vibrating sphere were also not investigated further. In units which responded to the vibrating sphere the receptive field was determined crudely by moving the vibrating sphere along the side of the fish and monitoring response strength by listening to the audiomonitor. The sphere was then placed where the strongest response (in some cases, the strongest reduction of neural activity) was elicited. With the sphere at this location, the unit's level-response function was measured in 2–5 dB steps in still water. For each displacement amplitude tested, unit responses to 20 repetitions of the 50 Hz stimulus, presented at a repetition rate of 0.4 Hz, were recorded. Then, water flow was initiated (flow velocity 15.5 cm s^{-1}) and the level-response function was measured in running water. Finally, the level-response function was measured again in still water to check that the unit's responsiveness had not changed. Then, the displacement amplitude was adjusted to 2700 μm p–p and the unit's response to the vibrating sphere was recorded in still water and in water running at flow velocities between 1.7 and 19.4 cm s^{-1}.

To measure unit responsiveness to running water, the non-vibrating sphere was placed at least 10 cm behind the fish and water flow was initiated by starting the motor driving the model ship's propeller. After approximately 10 s, neural activity was recorded for 60 s (20 consecutive data traces, each of 3 s duration), during which the water velocity remained constant. Then, flow velocity was increased to a higher value and unit activity was recorded again for 20×3 s. Using this protocol, unit activity was recorded with flow velocities between 1.7 and 19.4 cm s^{-1}.

To test for transient effects on unit responses caused by the onset and end of the water flow, unit activity was recorded for 1–2 min while the water was still, then flow was turned on and activity was recorded for another 2–4 min, after which the motor driving the model ship's propeller was turned off and unit activity was recorded for an additional 2–4 min.

Data analysis

Data were obtained from 46 lateral line units. Responses to the vibrating sphere were quantified by the average firing rates (spikes s^{-1}) during sphere vibration, the average phase angle (degrees) of each spike with respect to the signal delivered to the vibrator, the degree of phase-locking (synchronization coefficient R) and the Rayleigh statistic Z. Average firing rate was determined from the number of spikes elicited during the 20 stimulus presentations and compared with the average ongoing firing rate during a 1 s period, starting 1 s after sphere vibration had ended. Spike numbers during these 1 s periods were averaged across the 20 stimulus traces. Previous measurements of the water motions generated by our vibrating sphere showed that the time waveforms of the water motions reproduced the electrical signal that was delivered to the vibrator and that water motions after stimulus end did not last longer than approximately 200–300 ms (Plachta et al., 1999).

The time of occurrence of each action potential during stimulus presentation was determined with respect to each cycle of the 50 Hz signal and used to calculate the corresponding phase angles. From these data, the mean phase angle and the synchronization coefficient R (vector strength, after Goldberg and Brown, 1969) were calculated. The direction of the vector describes the average phase angle to which a unit responds and its magnitude describes the strength of phase-locking. A vector strength of 1 indicates that all spikes occured at the same phase angle. The Rayleigh statistic Z was used to determine whether measures of vector strength were statistically significant: $Z=R^2N$, where N=total number of spikes (Batschelet, 1981). Z values above 4.6 indicate a probability of 0.01 or less that spikes were randomly distributed during a vibration cycle.

To further characterize unit responses, the slopes of the level-response functions (ongoing rates subtracted) were determined at the steepest part of each function. To determine threshold, evoked rates (ongoing rates subtracted) were normalized and threshold was defined as the displacement amplitude that elicited 10 % of the maximum response when a unit responded with an increased rate, or 10 % of the minimum response when a unit responded with a decreased rate.

In 30 units, responses to running water were quantified by the average firing rates (spikes s^{-1}) during each 60 s period of constant water velocity (see Stimulation protocol). To compare neural activity in still and running water, the number of spikes during each 3 s trace was determined. Spike counts for the 20 traces that were recorded at a given water velocity were compared with spike counts for 20 traces recorded in still water

(Wilcoxon-test, $P \leq 0.01$). 16 units were lost before this test was completed, and their responses to running water were quantified by the units' ongoing activity in running water (see above) with the vibrating sphere (2700 µm displacement) placed 6–7 mm away from the fish. Units were defined as flow-sensitive if discharge rates increased or decreased with increasing flow velocity and, from a particular unit-specific flow velocity on, were significantly different ($P \leq 0.01$) from the discharge rates in still water. In three units, which were clearly flow-sensitive at velocities between 4 and 12 cm s^{-1}, discharge rates in running water were comparable to those in still water at the highest flow velocities tested.

For each unit, discharge rates measured in the presence of a constant water flow were plotted as a function of flow velocity and a linear regression was fitted to the data (data points above rate saturation were excluded). The slope of the regression line was used as a measure of the degree of flow sensitivity (Fig. 1A).

One unit apparently did not show increased or decreased activity in the presence of a constant water flow. However, plotting the peri-stimulus time (PST) histogram (bin width 1 s) revealed a transient response to the onset of the water flow. The unit was thus considered flow-sensitive.

Masking of responses to the vibrating sphere

To determine whether the responses of a given unit to the vibrating sphere were affected by running water, level-response functions measured in still and running water were compared. For this analysis, ongoing discharge rates were subtracted from stimulus-evoked discharge rates. Firing rates and synchronization coefficients (R values) were then plotted as a function of sphere displacement and linear regressions were fitted to the data (Fig. 1B,C). Data points below threshold and above saturation and R values that were not statistically significant ($Z \leq 4.6$) were omitted for this analysis. Regressions obtained under still and running water conditions were compared by analysis of covariance (ANCOVA, $P \leq 0.01$). Responses to the vibrating sphere in running water were defined as masked if the regression fitted to firing rates or to the synchronization coefficients or both had shallower slopes or were shifted towards lower values compared to the corresponding regressions in still water.

To determine the degree of masking, level-response functions for both spike rates (ongoing rates subtracted) and synchronization coefficients were integrated (Fig. 1B,C). Integrals of response functions measured in running water were expressed as a percentage of the integrals of response functions measured in still water. In a few cases this method yielded negative percentages because the ongoing rates in running water, on average, were slightly greater than evoked rates. Since in these cases masking was complete, the per cent integral was set to zero.

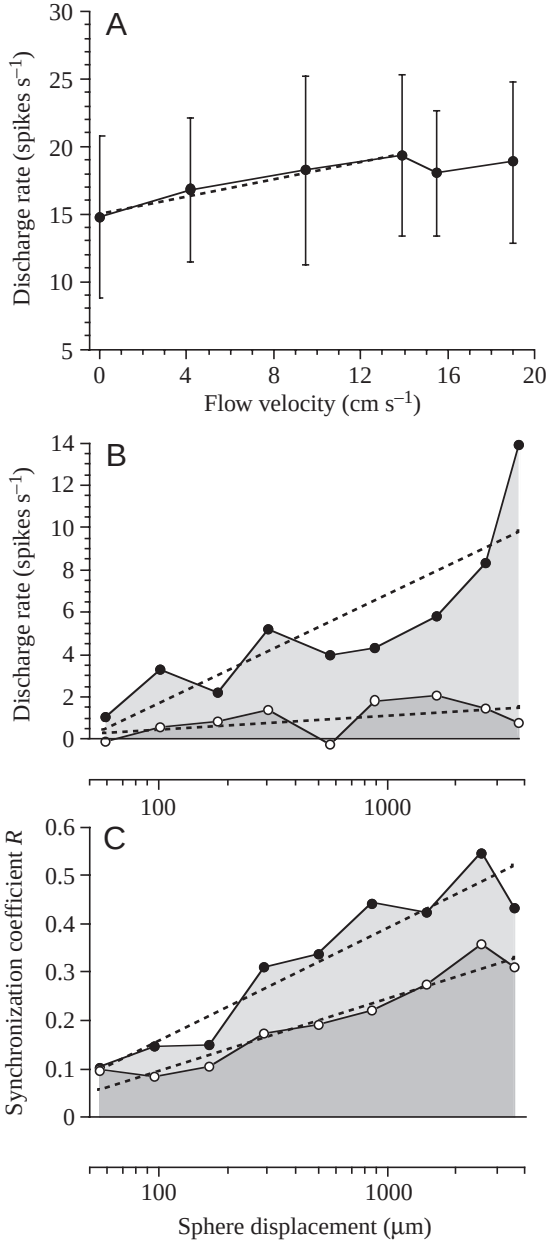

Fig. 1. Measures used to quantify medial octavolateralis nucleus (MON) unit responses. (A) Sensitivity to running water. Discharge rate, mean ± S.D. averaged across 60 s of constant water velocity (ongoing rate subtracted), of a MON unit is plotted as function of flow velocity. A linear regression was fitted to the data (broken line) and was used as a measure of flow sensitivity. (B) Level-response function of a MON unit. Mean discharge rate (ongoing rate subtracted) is plotted as function of sphere displacement in still (filled circles, averaged across 20 stimulus presentations) and running (open circles) water. (C) Strength of phase-locking of a MON unit. Synchronization coefficients R are plotted as function of sphere displacement in still (filled circles) and running (open circles) water. Linear regressions (broken lines) were fitted to the data shown in B and C and compared by analysis of covariance (ANCOVA) to determine whether responses were masked in running water. To determine the degree of masking, the areas under the functions shown in B and C were calculated. Areas under the curves obtained from measurements in running water (dark shaded areas) were expressed as a percentage of the area under the curves obtained from measurements in still water (light shaded areas).

Five units were lost before level-response functions in still and running water were completely measured. In these units, regression analysis was not possible and masking was determined by comparing firing rates in response to a given displacement amplitude in still and running water using the Wilcoxon-test ($P \leq 0.01$).

To test for differences between unit populations (see Results), regression line slopes and per cent integrals were compared using the Mann–Whitney *U*-test for independent samples ($P \leq 0.01$).

Verification of recording sites

In 11 fishes, a total of 19 electrolytic lesions were placed at physiologically characterized recording sites by passing a small current for 26 s through the electrode tip. Fish were deeply anesthetized with MS-222 (tricaine methane sulfonate) and perfused intracardially with a physiological salt solution (Oakley and Schafer, 1978) followed by 4 % glutaraldehyde solution in 0.1 mol l^{-1} phosphate buffer (pH 7.4). Brains were removed, postfixed and cut at 15 µm in a transverse plane parallel to the electrode penetrations. Sections were stained with Cresyl-Violet, analyzed under a microscope and lesions reconstructed with the aid of a computer (Macintosh PPC) and Photoshop 4.0 software. 17 lesioned recording sites were identified in transverse sections of the brain. All lesions were located dorsally in the MON, just below the cerebellar crest, indicating that recordings were made in the crest cell layer (New et al., 1996). Representative sections through the brainstem of a goldfish with a lesion in the MON have been published previously (e.g. Mogdans and Goenechea, 2000; Mogdans and Kröther, 2001).

Results

Responses to the vibrating sphere in still water

In still water, 37 units responded to the vibrating sphere with an increase and five units with a decrease in discharge rate. Two other units responded with both an increase and a decrease in discharge rate, depending on the location of the sphere along the side of the fish. Finally, for two units, discharge rate during sphere vibration was not different from ongoing discharge rate. However, these units responded to the vibrating sphere with phase-coupled discharges. On average, displacement amplitudes of 250 µm p–p were necessary to elicit a neural response. In some cases, especially among units that responded with a reduction in discharge rate, displacement amplitudes at threshold were even greater (Table 1).

Table 1. *Response characteristics of 46 medullary lateral line units to a vibrating sphere in still water*

	Mean±S.D.	Range
Ongoing rate (spikes s^{-1})	11.4±7.0	0–24
Maximum evoked rates (spikes s^{-1})	20.1±9.5	5.1–39.6
Maximum synchronization coefficient *R*	0.56±0.2	0.1–0.87
Rate threshold (µm sphere displacement)	250±240	4–1000
Rate-level slope (spikes s^{-1} per 10 dB)	4.4±2.3	1.5–11.6

Analysis of PST histograms revealed a variety of patterns comparable to those described previously (Mogdans and Goenechea, 2000; Mogdans and Kröther, 2001). If displacement values were used that caused rate saturation, responses were either sustained for the duration of the stimulus (N=20) or adapting (N=24), i.e. after an initial response peak, discharge rates returned to pre-stimulus levels. 30 units had robust phase-locking, $R > 0.5$. In 16 units, phase-locking was rather weak, $R \leq 0.5$. Due to fairly shallow rate-level slopes, on

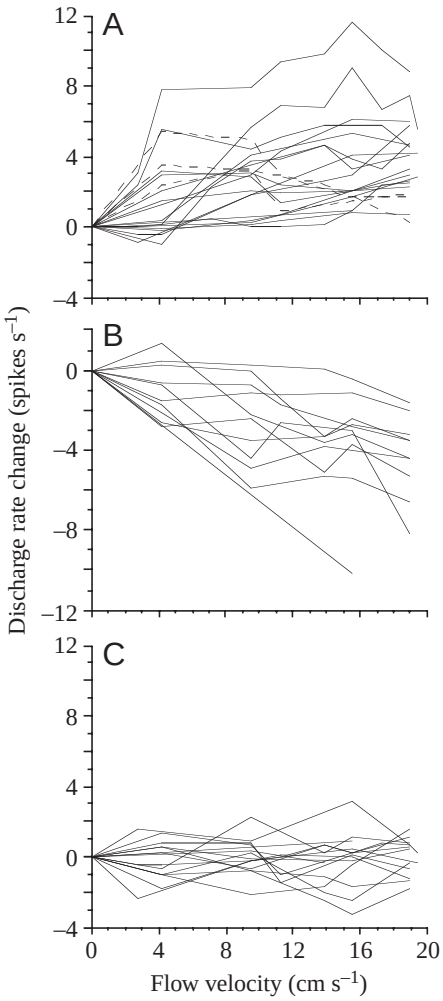

Fig. 2. Sensitivity of medial octavolateralis nucleus (MON) units to running water. Change in discharge rate is plotted as a function of flow velocity. A rate change of zero indicates that discharge rates in still and running water were identical. (A) Data from flow-sensitive units that responded with increasing ongoing discharge rates to increasing flow velocities. Broken lines represent data from units in which discharge rates decreased at flow velocities above approx. 10 cm s^{-1}. (B) Data from flow-sensitive units that responded with decreasing discharge rates to increasing flow velocities. (C) Data from flow-insensitive units. In these units, ongoing discharge rate in still water was not different from the ongoing rates measured at any of the tested flow velocities.

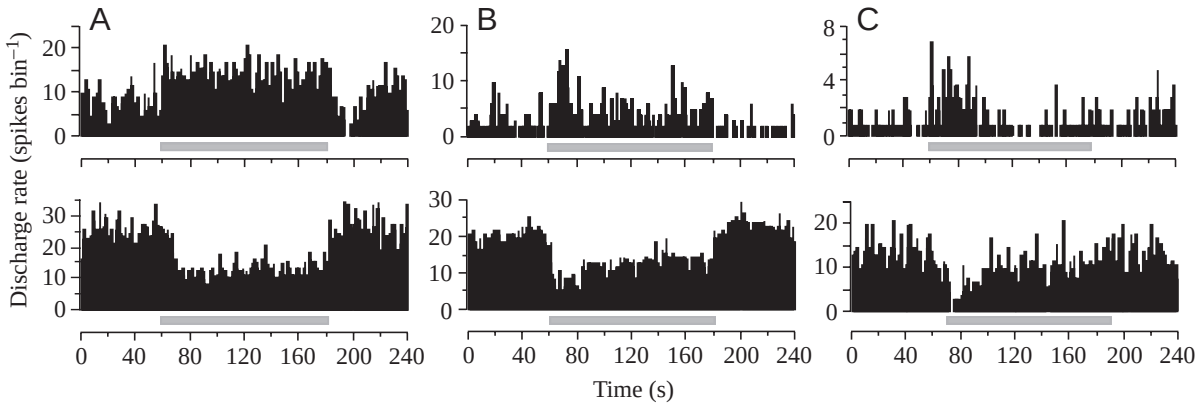

Fig. 3. Peri-stimulus time histograms (bin width 1 s) of the activity of single medial octavolateralis nucleus (MON) units stimulated with a water flow of 15.5 cm s^{-1}. The horizontal bar below each diagram indicates flow duration. (A) Examples of two units that showed sustained increases (top) and decreases (bottom) in discharge rate as long as the water was flowing. (B) Examples of two units that showed increases (top) and decreases (bottom) in discharge rate that were more strongly pronounced during a transient period shortly after flow onset than for the remaining time of water flow. (C) Example of two units that responded to the onset of water flow with a transient increase (top) or decrease (bottom) in discharge rate.

average, maximum evoked rates were only approximately twice as large as ongoing rates (Table 1).

Sensitivity to running water

Sensitivity to running water was determined by recording ongoing unit activity in running water with the non-vibrating sphere placed 10 cm behind the fish. 31 units (67 %) were flow-sensitive, i.e. ongoing rates in running water were significantly different from those in still water. In 17 of these units discharge rate increased (Fig. 2A), and in 11 units discharge rate decreased with increasing water velocity (Fig. 2B). In three units, discharge rate initially increased with increasing water velocity to a maximum and then decreased (Fig. 2A, broken lines). 15 units (33 %) did not respond to running water at any of the velocities tested and were thus considered flow-insensitive (Fig. 2C).

Transient effects caused by the onset and end of water flow were studied in 12 units. In 10 units, discharge rates increased (N=6) or decreased (N=4) shortly after water flow was initiated and remained at an elevated (or reduced) level of activity for the time period during which water was flowing (Fig. 3A). In three of these units, increases and decreases in discharge rate were more strongly pronounced during a transient period shortly after flow onset than during the remaining time of water flow (Fig. 3B). When the water flow was turned off, discharge rates returned to levels that were comparable to those in still water. One unit responded to the onset of water flow with a transient increase, and another with a transient decrease in

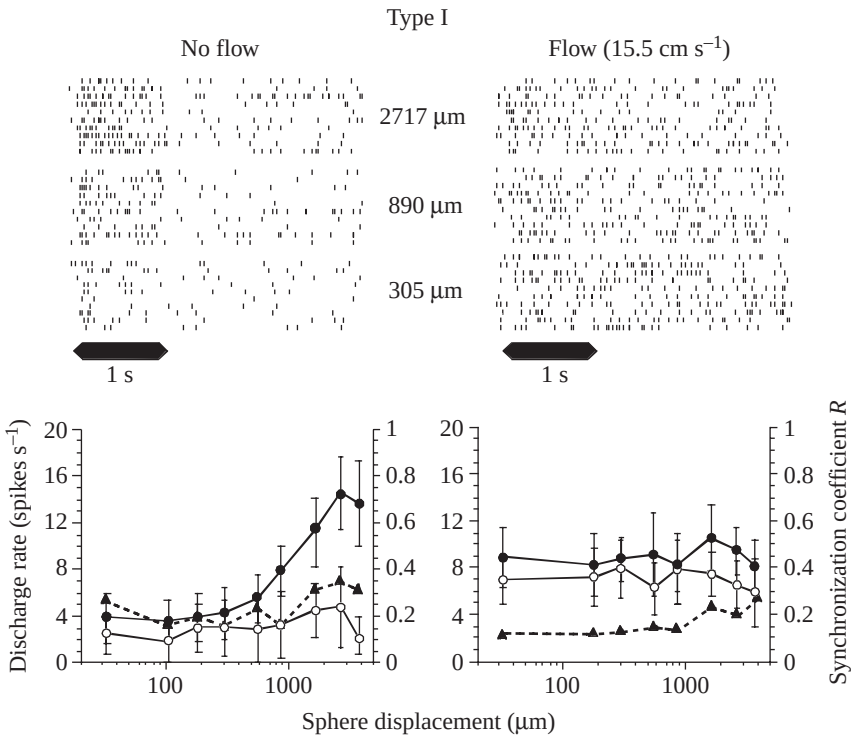

Fig. 4. Responses of a type I medial octavolateralis nucleus (MON) unit to a 50 Hz vibrating sphere stimulus in still (left) and running (15.5 cm s^{-1}; right) water. (Top) Raster plots of the responses to 10 stimulus repetitions for three displacement amplitudes (2717, 890 and 305 µm) (see also Figs 5–8). The stimulus trace is shown below the rasters. (Bottom) Level-response functions. Evoked discharge rates (means ± S.D.) (filled circles), averaged across 20 stimulus presentations, ongoing discharge rates (open circles) and synchronization coefficients (triangles) are plotted as function of sphere displacement. In still water, this unit responded to the vibrating sphere with an increase in discharge rate. In running water, the unit's ongoing discharge rate was increased. Consequently, the response to the vibrating sphere was masked both in terms of spike rate and phase-coupling.

discharge rate, i.e. neural activity returned to still-water levels while the water was still flowing (Fig. 3C).

Responses to the vibrating sphere in running water

Three main types of units were distinguished on the basis of their responses to running water and the masking of the responses to the vibrating sphere by running water.

Type I units (N=27) were flow-sensitive, i.e. they exhibited increased or decreased levels of activity in running water (see Fig. 2A,B). The responses of type I units to the vibrating sphere were masked by runnning water either in terms of spike rate (N=17) or both spike rate and phase-coupling (N=10). In Fig. 4, data are shown from a type I unit that responded to the vibrating sphere in still water with an increase in discharge rate. With increasing displacement amplitude of the vibrating sphere, the number of spikes increased, whereas the degree of phase-locking to the stimulus (synchronisation coefficient R) remained low (Fig. 4, left). In running water, ongoing discharge rate was increased. The response to the vibrating sphere, however, was no longer apparent (Fig. 4, right). Consequently, level-response functions measured in running water differed from those measured in still water in terms of both spike rate and phase-locking.

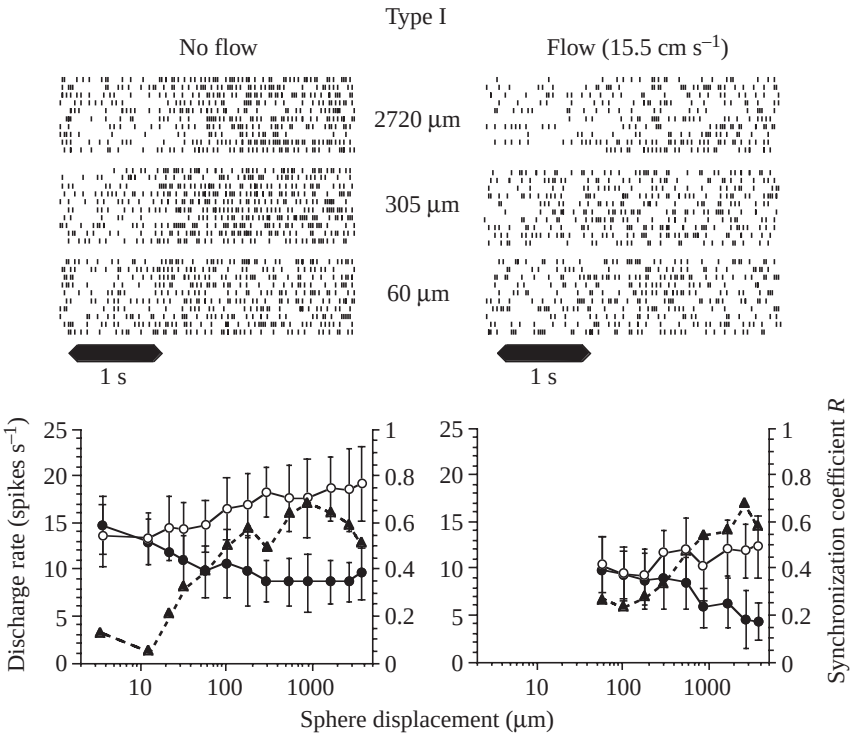

Fig. 5. Responses of a type I medial octavolateralis nucleus (MON) unit to a 50 Hz vibrating sphere stimulus in still (left) and running (15.5 cm s^{-1}; right) water. Raster plots and level-response functions are as in Fig. 4. Displacement amplitudes were 2720, 305 and 60 μm. In still water, the unit responded to the vibrating sphere with a decrease in discharge rate. In running water, the unit's ongoing discharge rate was decreased (sphere displacements <60 μm were not tested). As a consequence, the response to the vibrating sphere was masked in terms of spike rate. Phase-coupling was comparable in still and running water.

Data from another type I unit are shown in Fig. 5. This unit responded to the vibrating sphere in still water with a decrease in discharge rate (Fig. 5, left). With increasing displacement amplitude, the number of spikes during stimulus presentation decreased, even though phase-locking to the stimulus increased. In running water, ongoing discharge rate was reduced compared to still water conditions. As a consequence the decrease in discharge rate in response to the vibrating sphere was apparent only at displacements greater than 100 μm (Fig. 5, right). Thus, in this unit, the level-response function measured in running water differed from that measured in still water, both in terms of spike rate and phase-locking.

Type II units (N=7) were flow-insensitive, i.e. they did not respond to running water (e.g. Fig. 2C). In addition, the responses of type II units to the vibrating sphere were not masked in any respect by running water. Data from a type II unit are shown in Fig. 6. This unit responded to the vibrating sphere in still water with an increase in discharge rate (Fig. 6, left). With increasing displacement amplitude, both the number of spikes during stimulus presentation and the degree of phase-locking to the stimulus increased. In running water, ongoing discharge rate, evoked discharge rate and phase-locking to the vibrating sphere stimulus were not different from the respective values in still water (Fig. 6, right).

Data from another type II unit are shown in Fig. 7. This unit responded to the vibrating sphere in still water with a decrease in discharge rate (Fig. 7, left). With increasing displacement amplitude of the vibrating sphere, the number of spikes during stimulus presentation decreased. Phase-coupling was low for all displacement amplitudes applied. As in the previous example, ongoing discharge rate, evoked discharge rate and phase-locking in running water were not different from the respective measurements in still water (Fig. 7, right).

Type III units (N=7) were, like type II units, flow-insensitive. However, in contrast to type II units, the responses of type III units to the vibrating sphere stimulus were masked in running water either in terms of spike rate (N=2), or in terms of phase-coupling (N=3), or both (N=2). Data from a type III unit are shown in Fig. 8. The unit responded to the vibrating sphere in still water with an increase in discharge rate (Fig. 8, left). With increasing displacement amplitude of the vibrating sphere, both the number of spikes during stimulus presentation and the degree of phase-locking to the stimulus increased. Ongoing activity in running water was not different from the rate in still water (Fig. 8, right). Nevertheless, discharge rate and phase-coupling to the vibrating sphere stimulus in running water were lower than under still-water conditions.

Fig. 9 summarizes the differences between type I, type II and type III units. Firstly, all type I units were flow-sensitive whereas type II and type III units were not. This is evident from a comparison of the absolute slopes of the regression lines that were used as a measure of flow-sensitivity (see Materials and methods). Median slopes were 0.33 spikes cm^{-1} per $cm\,s^{-1}$ increase in flow velocity (range 0.01–0.73), 0.06 spikes cm^{-1} per $cm\,s^{-1}$ (range 0.004–0.07) and 0.04 spikes cm^{-1} per $cm\,s^{-1}$ (range 0.008–0.23) for type I, type II and type III units, respectively (Fig. 9A). The slopes of type I units were significantly greater than those of type II and type III units (Mann–Whitney *U*-test, $P<0.001$). The slopes of the regression lines of type II units were not different from those of type III units ($P=0.34$). Secondly, the responses of type I and type III units to the vibrating sphere were masked in running water, whereas the responses of type II units were not different in still and running water. This is evident by comparing the integrals of the level-response functions in running water with those in still water. This measure was used to quantify the degree of masking (see Materials and methods). In terms of spike rate, median integrals of type I, II and III units in running water were 21 % (range 0–58 %), 108 % (range 101–125 %) and 29 % (range 6–96 %) of the integrals in still water (Fig. 9B). The percentages obtained from type II units were different from those obtained from type I and type III units (*U*-test, $P<0.001$). The percentages from type I units were not different from those of type III units ($P=0.29$). In terms of phase-coupling, similar results were obtained. Median integrals of type I, II and III units in running water were 77 % (range 45–117 %), 92 % (range 78–117 %) and 73 % (range 35–129 %) of the integrals in still water. Masking of phase-coupling was weaker than masking of spike rate. The statistical

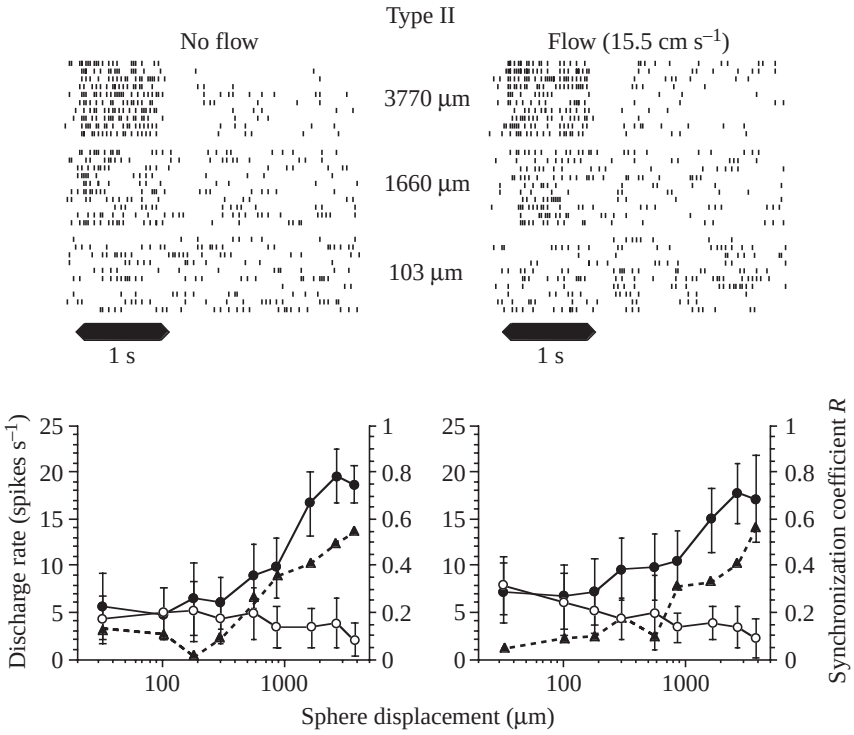

Fig. 6. Responses of a type I medial octavolateralis nucleus (MON) unit to a 50 Hz vibrating sphere stimulus in still (left) and running (15.5 $cm\,s^{-1}$; right) water. Raster plots and level-response functions are as in Fig. 4. Displacement amplitudes were 3770, 1660 and 103 µm. In still water, the unit responded to the vibrating sphere with an increase in discharge rate. Ongoing discharge rate was comparable in still and running water. Consequently, the response to the vibrating sphere was not masked.

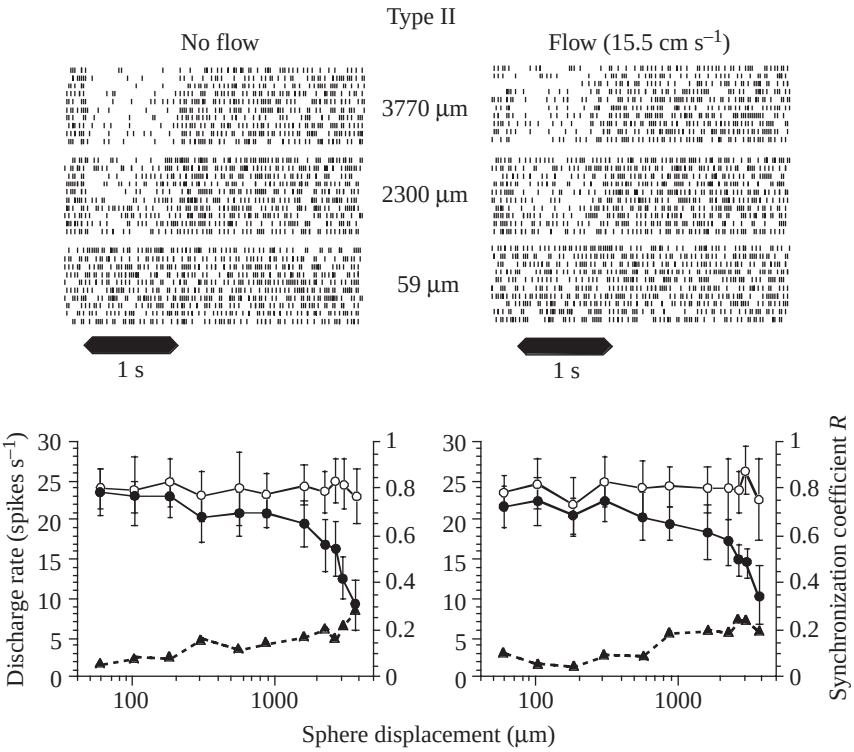

Fig. 7. Responses of a type I medial octavolateralis nucleus (MON) unit to a 50 Hz vibrating sphere stimulus in still (left) and running (15.5 $cm\,s^{-1}$; right) water. Raster plots and level-response functions are as in Fig. 4. Displacement amplitudes were 3770, 2300 and 59 µm. In still water, this unit responded to the vibrating sphere with a decrease in discharge rate. Ongoing discharge rate was comparable in still and running water. Consequently, the response to the vibrating sphere was not masked.

analysis did not yield significance (type II *versus* type I, P=0.032; type II *versus* type III, P=0.11), but masking was nevertheless evident (Fig. 9C). The percentages from type I units were not different from those of type III units (P=0.84).

Five units had response properties different from those of the three main unit types described above. Data from one of these units are shown in Fig. 10. In this unit, ongoing discharge rate increased in the presence of running water (flow-sensitive unit). Moreover, the discharge rate elicited by the vibrating sphere was also increased in running water. Consequently, the response to the vibrating sphere was not masked by running water. However, in terms of phase-coupling, the unit's response was masked. Data from the second unit are shown in Fig. 11. In still water, the unit responded to the vibrating sphere with an increase in discharge rate. In the presence of running water, ongoing discharge rate was decreased (flow-sensitive unit). Nevertheless, responses to the vibrating sphere were comparable in still and running water, at least for large displacement amplitudes. Consequently, the ratio between evoked and ongoing discharge rate was increased in running water. The third unit responded with an increase in discharge rate in response to the vibrating sphere (data not shown). In running water, ongoing discharge rate was slightly increased (flow-sensitive unit). Nevertheless, the unit's response to the vibrating sphere was not masked in running water. The fourth unit (data not shown) responded only to the onset of water flow with a transient increase of discharge rate. Consequently, the response to the vibrating sphere was not masked. In the fifth unit, masking of the response to the vibrating sphere by running water depended on sphere location (see below and Fig. 12C).

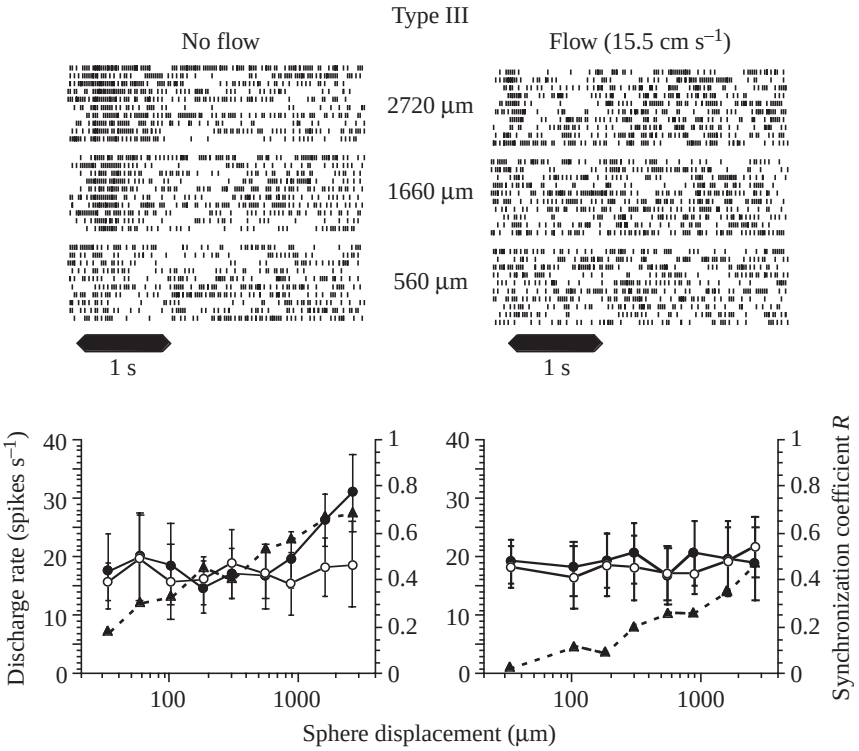

Fig. 8. Responses of a type I medial octavolateralis nucleus (MON) unit to a 50 Hz vibrating sphere stimulus in still (left) and running (15.5 cm s^{-1}; right) water. Raster plots and level-response functions are as in Fig. 4. Displacement amplitudes were 2720, 1660 and 560 μm. In still water, this unit responded to the vibrating sphere with an increase in discharge rate. Ongoing discharge rates in still and running water were comparable. Nevertheless, the response to the vibrating sphere was masked both in terms of spike rate and phase-coupling.

Masking of responses to the vibrating sphere at different receptive field locations

The main goal of this study was to investigate the effects of running water on unit responses to a stationary sphere. Therefore, receptive fields were not measured in detail. However, a crude analysis revealed that many units had receptive fields that consisted of a region from which stimulation with the vibrating sphere caused an increase in discharge rate (excitatory region) and another region from which stimulation with the vibrating sphere caused a decrease in discharge rate (inhibitory region) (Mogdans and Kröther, 2001). In eight units, the effect of running water was measured with the sphere positioned at two different locations within the receptive field.

In five units the response to the vibrating sphere was masked in running water, but masking did not depend on the location of the sphere. Data from one such unit are shown in Fig. 12A. In still water, stimulation with the vibration sphere in the head region caused a decrease, whereas stimulation near the trunk caused an increase, in discharge rate. In running water, both the inhibitory and the excitatory responses were masked. In two units, responses to the vibrating sphere were not masked in running water, and again the effect was independent of sphere location. Data from one such unit are shown in Fig. 12B. In still water, stimulation with the vibrating sphere near the caudal peduncle and in the trunk region caused an increase in discharge rate. Neither of these responses was masked in running water.

One unit was recorded in which masking depended on the location of the sphere within the receptive field (Fig. 12C). In still water, this unit responded with an increase in discharge rate when the sphere was placed near the operculum. In running water, the response was not masked. When the vibrating sphere was near the tip of the snout, the unit responded with a decrease in discharge rate, but in contrast to the previous location, the response was masked in running water.

Discussion

This is the first study to describe the responses of central lateral line neurons to a stationary dipole stimulus presented in running water. All previous studies on the responses of central lateral line neurons to hydrodynamic stimuli such as vibrating spheres (Coombs et al., 1998; Montgomery et al., 1996) and moving objects (Bleckmann and Zelick, 1993; Mogdans et al., 1997; Müller et al., 1996) have been performed in still water. In nature, conditions when the water surrounding a fish is absolutely still are rare. Normally the fish moves, the water moves, or both fish and water are moving. To understand how the lateral line functions under natural conditions, it is necessary to study the system in the presence of both still and running water. The data presented in this study describe the effects of d.c. water flow on the discharges of single lateral line units in the medial octavolateralis nucleus (MON) of the goldfish *Carassius auratus*.

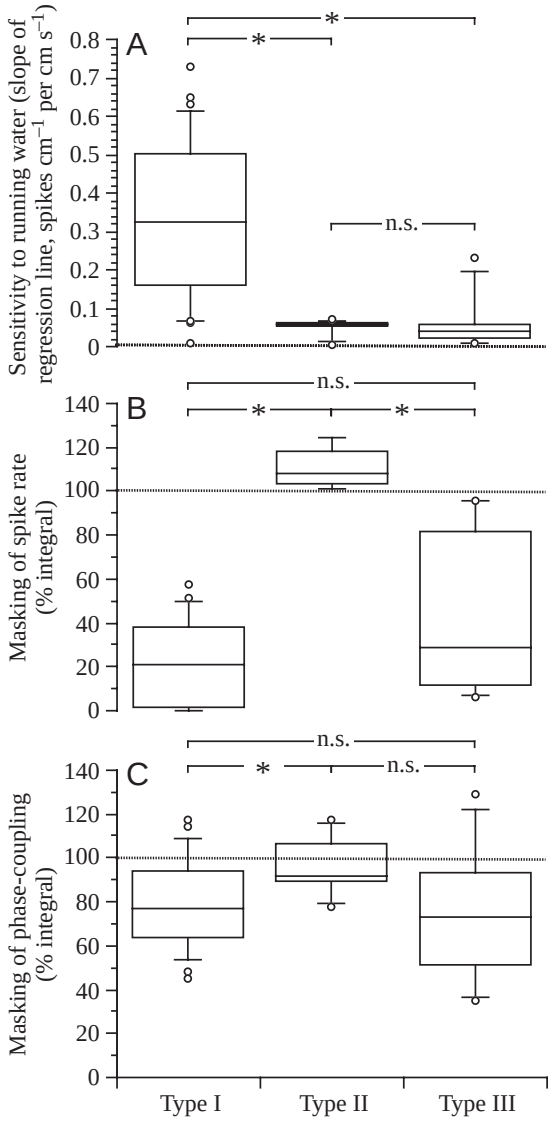

Fig. 9. Summary of the characteristics of type I, type II and type III units. Box-and-whisker plots are shown representing median values and 10, 25, 75 and 90 percentiles as well as data points below the 10th percentile and above the 90th percentile. (A) Slopes of regression lines fitted to flow-response functions (see Fig. 1A). (B) Masking of dipole-evoked discharge rate in running water. Integrals of rate-level functions measured in running water are expressed as percentage integrals of rate-level functions measured in still water (see Fig. 1B). (C) Masking of phase-coupling to the vibrating sphere. Integrals of response functions measured in running water are expressed as percentage integrals of response functions measured in still water (see Fig. 1C). Asterisks indicate statistically significant differences (*U*-test, $P \leq 0.05$). n.s., no difference ($P > 0.05$).

Flow-sensitive and flow-insensitive cells in the MON

Comparing ongoing activity of MON cells in still and running water allowed us to distinguish between flow-sensitive (type I) and flow-insensitive (type II and type III) units. In this respect, MON cells were comparable to primary lateral line afferents, which are also either sensitive (type I) or insensitive (type II) to running water (Engelmann et al., 2000; Voigt et al., 2000). Flow-sensitive afferents of type I probably innervate superficial neuromasts, whereas flow-insensitive type II afferents probably innervate canal neuromasts (Engelmann et al., 2000). Thus, it is tempting to speculate that flow-sensitive cells in the MON receive input predominantly from fibers innervating superficial neuromasts and that flow-insensitive MON cells receive input predominantly from fibers innervating canal neuromasts.

Flow-sensitive afferent fibers always responded to running water with a burst-like increase in discharge rate (Engelmann et al., 2000). This was probably because even a laminar water flow generated micro-turbulences close to the skin of the fish. Since we used an almost identical tank to the one in that study, comparable micro-turbulences must have been present. Nevertheless, MON cells did not show burst-like activity in running water. In addition, more than one-third of our flow-sensitive MON cells responded with a decrease in discharge rate to running water (Fig. 2). There are at least two explanations for this: (i) the peripheral effects caused by micro-turbulences are filtered at the level of the MON through an as-yet-unknown central mechanism, and/or (ii) a reduction of ongoing discharge rate in running water is due to inhibitory inputs onto MON cells mediated by interneurons (New et al., 1996).

Two MON cells responded only for 1 or 2 min after flow onset (Fig. 3C). Measurements with a constant-temperature anemometer showed that a constant water velocity in the flow tank was reached within approximately 10 s after the ship' propeller was turned on, so these cells did not respond to the water acceleration associated with the onset of the water flow. Perhaps these neurons were filtering stimuli of long duration. Neurons with such properties are suited to cancel unwanted responses to background flow information generated, for instance, in swimming fish. Previous studies have demonstrated the ability of MON cells for adaptive cancellation of responses to stimuli coupled to the fish's own ventilatory movements (Montgomery and Bodznick, 1994).

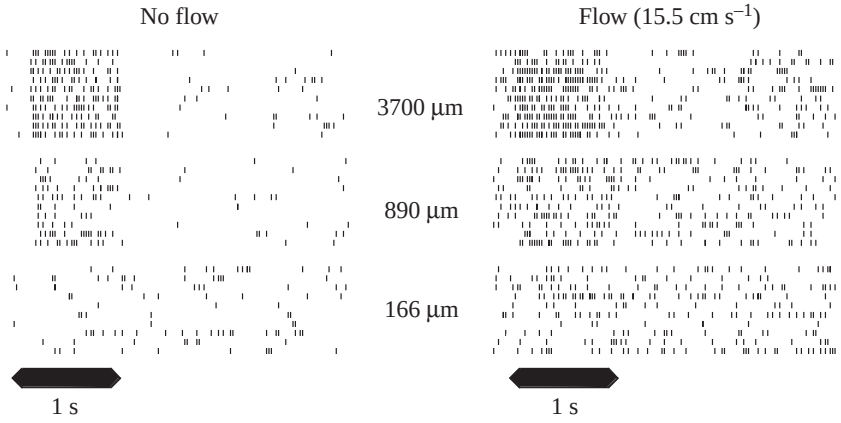

Fig. 10. Responses of a type I medial octavolateralis nucleus (MON) unit to a 50 Hz vibrating sphere stimulus in still (left) and running (15.5 cm s^{-1}; right) water. Raster plots are as in Fig. 4. Displacement amplitudes were 3700, 890 and 166 μm. In still water, the unit responded to the vibrating sphere with an increase in discharge rate. In running water, the unit exhibited both increased ongoing and increased evoked discharge rates.

Effects of running water on MON unit responses to a vibrating sphere

The responses of type I MON units to a vibrating sphere were masked in running water in terms of spike rate, or both spike rate and phase-coupling. Thus, the responses of type I MON cells were comparable to the dipole responses of type I afferent fibers, which are also masked by running water (Engelmann et al., 2000). This further supports the idea that type I MON cells receive input from type I afferents and thus process hydrodynamic information received by superficial neuromasts.

The responses of type II MON cells to a vibrating sphere were not masked in running water. Spike rates and phase-coupling were comparable in still and running water. Thus the responses of type II MON cells were comparable to the dipole responses of type II afferents, which are not masked by running water (Engelmann et al., 2000). This supports the assumption that type II MON cells receive input from type II afferent fibers and thus process hydrodynamic information received by canal neuromasts.

Theoretically, type II MON responses may result from the processing of input from a superficial neuromast with a vertical orientation, i.e. perpendicular to the direction of the flow. This neuromast should not respond to flow, provided that the flow is perfectly laminar. It should, however, still respond to a vibrating sphere, as this stimulus has spatial non-uniformities in the vertical dimension. Consequently, a central cell receiving input from this neuromast would be flow-insensitive and not masked, i.e. it would behave like a cell receiving input from a canal neuromast.

The responses of type III MON cells to a vibrating sphere were masked in running water even though these cells were flow-insensitive. Thus, type III cells had response properties intermediate between those of type I and type II cells. This can be explained if type III cells received input from both type I and type II afferents, i.e. if superficial and canal neuromast input converged at the level of the MON. Excitatory input from type II afferents (canal neuromasts) would explain why type III MON cells are flow-insensitive. Additional inhibitory input from type I afferents (superficial neuromasts) would explain the masking of type III MON responses. However, type III responses can also be explained by the processing of superficial neuromast information alone. A central cell may receive input from at least two oppositely oriented populations of hair cells located in different superficial neuromasts. In this case, the excitatory and inhibitory effects caused in the respective afferent fibers will be cancelled at the level of the central cell and the cell will thus be rendered flow-insensitive. Since the response to the vibrating sphere in running water is masked already at the level of the periphery (Engelmann et al., 2000), the central cell's response will also be masked.

Some units exhibited responses unlike those of the main three response types: they were flow-sensitive but the responses to the vibrating sphere were not masked in running water (Figs 10, 11). A plausible explanation for this behavior

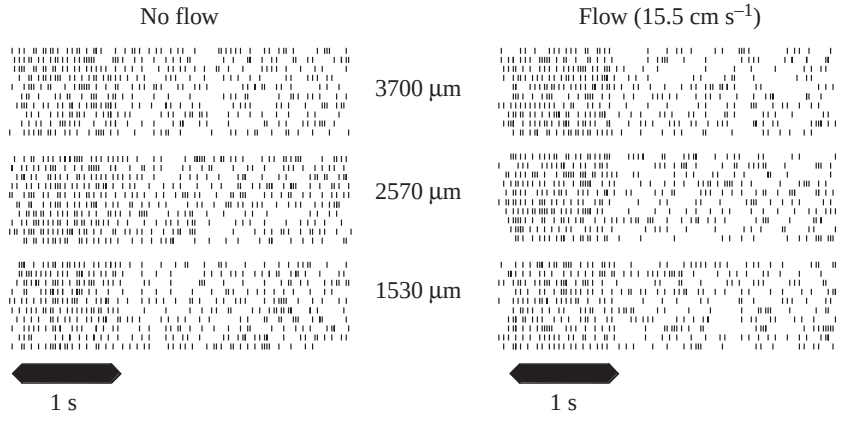

Fig. 11. Responses of a type I medial octavolateralis nucleus (MON) unit to a 50 Hz vibrating sphere stimulus in still (left) and running (15.5 cm s^{-1}; right) water. Raster plots are as in Fig. 4. Displacement amplitudes were 3700, 2570 and 1530 μm. In still water, the unit responded to the vibrating sphere with an increase in discharge rate. In running water, ongoing discharge rate was decreased. The responses to the vibrating sphere, however, were comparable in still and running water.

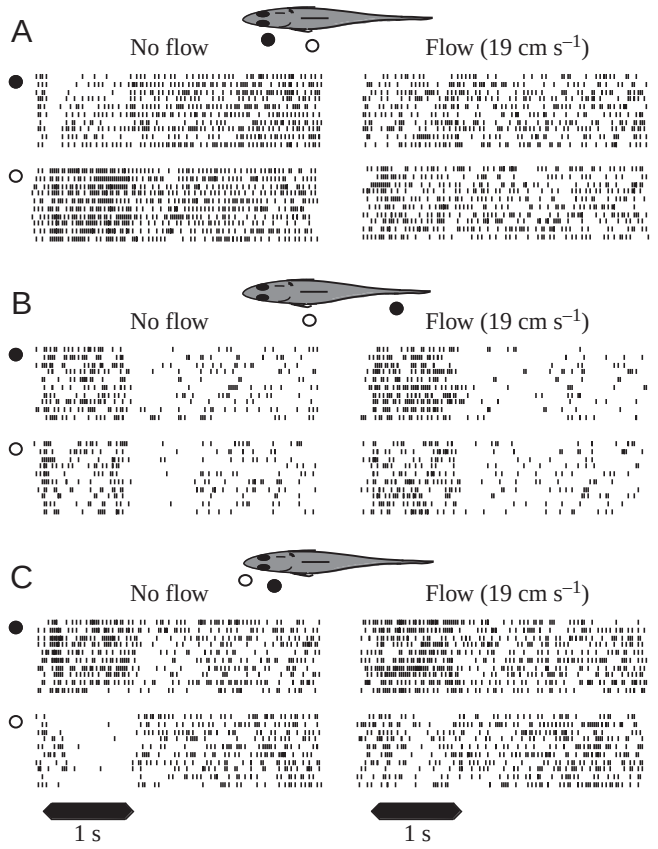

Fig. 12. Responses of three type I medial octavolateralis nucleus (MON) units to a 50 Hz vibrating sphere stimulus. Raster plots are shown of the responses to the sphere presented at two distinct locations along the side of the fish (indicated by open and filled circles). Displacement amplitude was 2717 µm. (A) Example of a unit that responded with a decrease in discharge rate when the sphere was in the head region and with an increase in discharge rate when the sphere was in the trunk region. Both responses were masked in running water. (B) Example of a unit that responded with an increase in discharge rate when the sphere was near the caudal peduncle and when the sphere was in the trunk region. Neither of these responses was masked in running water. (C) Example of a unit that responded with an increase in discharge rate when the sphere was opposite to the operculum and with a decrease in discharge rate when the sphere was near the tip of the snout. The response elicited by the sphere placed near the operculum was not masked, whereas that elicited by the sphere placed near the snout was masked by running water.

is that these units received excitatory input from both type I and type II afferents, i.e. from both superficial and canal neuromasts.

Eight units were held long enough to test the effects of running water on the responses elicited from two different sphere locations. In seven units responses were either masked or not masked, and were independent of sphere location, suggesting that these units received input from only one type of neuromast. However, we found one cell in which responses to the vibrating sphere were masked by running water in one part but not in another part of the receptive field. This suggests that this cell received information from both superficial neuromasts and canal neuromasts located in different parts of the lateral line periphery.

Central lateral line pathways

The peripheral lateral line exhibits a clear morphological and functional separation, having two types of receptive organs, the superficial and canal neuromasts, with different morphological and biomechanical properties (for reviews, see Bleckmann, 1994; Coombs and Montgomery, 1999). Behavioral data strongly suggest that the two types of neuromasts have different functions. Superficial neuromasts appear to be necessary for rheotaxis behavior (Baker and Montgomery, 1999; Montgomery et al., 1997). In contrast, canal neuromasts may mediate orienting behavior and thus may be essential for the localization of a hydrodynamic source (Coombs et al., 2001). This dual role of the two lateral line subsystems suggests a largely separate processing of superficial and canal neuromast information. In addition, all previous physiological studies indicated that superficial and canal neuromasts are innervated by different populations of afferent fibers (e.g. Kroese and Schellart, 1992; Coombs and Janssen, 1990; Coombs and Montgomery, 1992; Montgomery and Coombs, 1992; Wubbels, 1992), suggesting that information from superficial and canal neuromasts reaches the brain *via* separate channels. The data from the present study support the idea that the peripheral separation of superficial and canal neuromast input is largely maintained at the first site of sensory integration in the lateral line brainstem.

The idea that separate channels for the processing of superficial and canal neuromast input exist throughout the ascending lateral line pathway is further supported by studies in which a moving object was used as a lateral line stimulus (Mogdans and Bleckmann, 1998). Two types of primary afferents can be distinguished, based on their response to a moving object: fibers that respond with unpredictable bursts of activity to the wake generated by the moving object, and fibers that do not respond to the wake. Fibers of the first type probably innervate superficial neuromasts whereas fibers of the second type innervate canal neuromasts. In the brain, responses to moving objects similar to those in the periphery can be found. As seen both at the level of the medulla (Mogdans et al., 1997) and in the midbrain torus semicircularis (Wojtenek et al., 1998), one population of lateral line neurons responds with a short burst of activity to a passing moving object but not to the object's wake, whereas other neurons respond to the wake, which suggests that they process input from canal and superficial neuromasts, respectively.

Even though there is strong evidence for largely separate processing of superficial and canal neuromast information, interactions between the two subsystems cannot be ruled out. There are three possible candidates for the convergence of superficial and canal neuromast input at the level of the MON: (i) flow-insensitive type III units that have response properties intermediate to those of type I and II units (c.f. Fig. 8), (ii) flow-sensitive units that respond about equally well to the vibrating sphere in still and running water (cf. Figs 10, 11), and

(iii) units in which dipole responses are masked at one location in the receptive field but not at another (cf. Fig. 12C). In addition, both in the medulla and in the midbrain, many neurons exhibit responses to a moving object (Bleckmann and Zelick, 1993; Müller et al., 1996; Mogdans et al., 1997; Wojtenek et al., 1998), which can hardly be explained by processing input exclusively from superficial or from canal neuromasts.

Another aspect of hydrodynamic information processing by MON neurons deserves consideration. Whereas most MON cells readily respond to the complex water motions generated by a moving object, only a small proportion of MON cells responds to the water motions generated by a stationary vibrating sphere (Mogdans and Goenechea, 2000). Many MON cells that do respond to a vibrating sphere, do so only at vibration amplitudes that are substantially greater than those needed to elicit responses from primary afferents (e.g. Coombs et al., 1998; Engelmann et al., 2000; present study). Cells of the first type may be part of a pathway for the processing of complex hydrodynamic information that stimulates large parts of the lateral line periphery. In contrast, cells of the second type may be part of a pathway that processes local hydrodynamic information. However, this does not exclude the possibility that cells which respond to a stationary dipole stimulus are also involved in the processing of more complex water motions.

Finally, the understanding of hydrodynamic information processing by brainstem lateral line neurons is complicated by the fact that many MON cells receive input from both the anterior and the posterior lateral line, i.e. from afferent fibers that innervate neuromasts on both the head and the trunk. This can be seen in measurements of receptive fields that may extend from as far rostral as the tip of the snout to as far caudal as the tail fin (Coombs et al., 1998; Mogdans and Kröther, 2001). Stimulation in one part of the receptive field can be excitatory whereas stimulation in an adjacent part can be inhibitory (Mogdans and Kröther, 2001). Moreover, responses to hydrodynamic stimuli in running water may depend on the location of the stimulus within a unit's receptive field (this study). One of the challenges of lateral line research is to understand the intricate network that underlies the processing of hydrodynamic information in the fish brainstem.

We thank J. Engelmann for helpful comments on the manuscript. The research reported in this paper was performed under the guidelines established by current German animal protection law. Use of animals and experimental procedures were approved by Regierungspräsidium Köln, permission no. 23.203.2 BN 23. This research was supported by the DFG (Bl 242/10-1).

References

Baker, C. F. and Montgomery, J. C. (1999). The sensory basis of rheotaxis in the blind Mexican cave fish, *Astyanax fasciatus*. *J. Comp. Physiol. A* **184**, 519–527.

Batschelet, E. (1981). The Rayleigh test. In *Circular Statistics in Biology* (ed. E. Batschelet), pp. 54–58. New York: Academic Press.

Blaxter, H. S. and Fuiman, L. A. (1989). Function of the free neuromasts of marine teleost larvae. In *The Mechanosensory Lateral Line. Neurobiology and Evolution* (ed. S. Coombs, P. Görner and H. Münz), pp. 481–499. New York: Springer.

Bleckmann, H. (1994). Reception of hydrodynamic stimuli in aquatic and semiaquatic animals. In *Progress in Zoology*, vol. 41 (ed. W. Rathmayer), pp. 1–115. Stuttgart, Jena, New York: Gustav Fischer.

Bleckmann, H. and Zelick, R. (1993). The responses of peripheral and central mechanosensory lateral line units of weakly electric fish to moving objects. *J. Comp. Physiol. A* **172**, 115–128.

Coombs, S. and Janssen, J. (1990). Behavioral and neurophysiological assessment of lateral line sensitivity in the mottled sculpin, *Cottus bairdi*. *J. Comp. Physiol. A* **167**, 557–567.

Coombs, S. and Montgomery, J. C. (1992). Fibers innervating different parts of the lateral line system of an Antarctic Notothenioid, *Trematomus bernachii*, have similar frequency responses despite large variation in the peripheral morphology. *Brain Behav. Evol.* **40**, 217–233.

Coombs, S. and Montgomery, J. C. (1999). The enigmatic lateral line system. In *Comparative Hearing: Fish and Amphibians* (ed. R. R. Fay and A. N. Popper), pp. 319–362. New York: Springer.

Coombs, S., Mogdans, J., Halstead, M. and Montgomery, J. C. (1998). Transformation of peripheral inputs by the first-order lateral line brainstem nucleus. *J. Comp. Physiol. A* **182**, 609–626.

Coombs, S., Braun, C. B. and Donovan, B. (2001). The orienting response of lake Michigan mottled sculpin is mediated by canal neuromasts. *J. Exp. Biol.* **204**, 337–348.

Denton, E. J. and Gray, J. A. B. (1988). Mechanical factors in the excitation of the lateral lines of fishes. In *Sensory Biology of Aquatic Animals* (ed. J. Atema, R. R. Fay, A. N. Popper and W. N. Tavolga), pp. 595–617. New York: Springer.

Denton, E. J. and Gray, J. A. B. (1989). Some observations on the forces acting on neuromasts in fish lateral line canals. In *The Mechanosensory Lateral Line. Neurobiology and Evolution* (ed. S. Coombs, P. Görner and H. Münz), pp. 229–246. New York: Springer.

Engelmann, J., Hanke, W., Mogdans, J. and Bleckmann, H. (2000). Hydrodynamic stimuli and the fish lateral line. *Nature* **408**, 51–52.

Goldberg, J. M. and Brown, P. B. (1969). Response of binaural neurons of dog superior olivary complex to dichotic stimuli: some physiological implications. *J. Neurophysiol.* **3**, 613–636.

Hanke, W., Brücker, C. and Bleckmann, H. (2000). The ageing of low-frequency water disturbances caused by swimming goldfish and its possible relevance to prey detection. *J. Exp. Biol.* **203**, 1193–1200.

Harris, G. G. and van Bergeijk, W. A. (1962). Evidence that the lateral line organ responds to near-field displacements of sound sources in water. *J. Acoust. Soc. Am.* **34**, 1831–1841.

Harris, G. G., Frishkopf, L. S. and Flock, A. (1970). Receptor potentials from hair cells of the lateral line. *Science* **167**, 76–79.

Hassan, E. S. (1989). Hydrodynamic imaging of the surroundings by the lateral line of the blind cave fish *Anoptichthys jordani*. In *The Mechanosensory Lateral Line. Neurobiology and Evolution* (ed. S. Coombs, P. Görner and H. Münz), pp. 217–228. New York: Springer.

Hoekstra, D. and Janssen, J. (1985). Non-visual feeding behavior of the mottled sculpin, *Cottus bairdi*, in Lake Michigan. *Env. Biol. Fishes* **12**, 111–117.

Kroese, A. B. A. and Schellart, N. A. M. (1992). Velocity- and acceleration-sensitive units in the trunk lateral line of the trout. *J. Neurophysiol.* **68**, 2212–2221.

Matsushima, T., Takei, K., Kitamura, S., Kusunoki, M., Satou, M., Okumoto, N. and Ueda, K. (1989). Rhythmic electromyographic activities of trunk muscles characterize the sexual behavior in the Hime salmon (landlocked sockeye salmon, *Oncorhynchus nerka*). *J. Comp. Physiol. A* **165**, 293–314.

Mogdans, J. and Bleckmann, H. (1998). Responses of the goldfish trunk lateral line to moving objects. *J. Comp. Physiol. A* **182**, 659–676.

Mogdans, J. and Goenechea, L. (2000). Responses of medullary lateral line units in the goldfish, *Carassius auratus*, to sinusoidal and complex wave stimuli. *Zoology* **102**, 227–237.

Mogdans, J. and Kröther, S. (2001). Brainstem lateral line responses to sinusoidal wave stimuli in the goldfish, *Carassius auratus*. *Zoology* **104**, 153–166.

Mogdans, J., Bleckmann, H. and Menger, N. (1997). Sensitivity of central units in the goldfish, *Carassius auratus*, to transient hydrodynamic stimuli. *Brain Behav. Evol.* **50**, 261–283.

Mogdans, J., Wojtenek, W. and Hanke, W. (1999). The puzzle of

hydrodynamic information processing: how are complex water motions analyzed by the lateral line? *J. Eur. Morphol.* **37**, 195–199.

Montgomery, J. C. and Bodznick, D. (1994). An adaptive filter that cancels self-induced noise in the electrosensory and lateral line mechanosensory systems of fish. *Neurosci. lett.* **174**, 145–148.

Montgomery, J. C. and Coombs, S. (1992). Physiological characterization of lateral line function in the Antarctic fish *Trematomus bernacchii*. *Brain Behav. Evol.* **40**, 209–216.

Montgomery, J. C. and Hamilton, A. R. (1997). Sensory contributions to nocturnal prey capture in the dwarf scorpion fish (*Scorpaena papillosus*). *Mar. Fresh. Behav. Physiol.* **30**, 209–233.

Montgomery, J. C. and Coombs, S. (1998). Peripheral encoding of moving sources by the lateral line system of a sit-and-wait predator. *J. Exp. Biol.* **201**, 91–102.

Montgomery, J. C. and Bodznick, D. (1994). An adaptive filter that cancels self-induced noise in the electrosensory and lateral line mechanosensory systems of fish. *Neurosci. lett.* **174**, 145–148.

Montgomery, J. C., Coombs, S. and Janssen, J. (1994). Form and function relationships in the lateral line systems: Comparative data from six species of antarctic notothenioid fish. *Brain Behav. Evol.* **44**, 299–306.

Montgomery, J. C., Bodznick, D. and Halstead, M. (1996). Hindbrain signal processing in the lateral line system of the dwarf scorpionfish *Scopeana papillosus*. *J. Exp. Biol.* **199**, 893–899.

Montgomery, J. C., Baker, C. F. and Carton, A. G. (1997). The lateral line can mediate rheotaxis. *Nature* **389**, 960–963.

Müller, H. M., Fleck, A. and Bleckmann, H. (1996). The responses of central octavolateralis cells to moving sources. *J. Comp. Physiol. A* **179**, 455–471.

Münz, H. (1979). Morphology and innervation of the lateral line system in *Sarotherodon niloticus* L. (Cichlidae, Teleostei). *Zoomorphol.* **93**, 73–86.

Münz, H. (1985). Single unit activity in the peripheral lateral line system of the cichlid fish *Sarotherodon niloticus* L. *J. Comp. Physiol. A* **157**, 555–568.

New, J. G., Coombs, S., McCormick, C. A. and Oshel, P. E. (1996). Cytoarchitecture of the medial octavolateralis nucleus in the goldfish, *Carassius auratus*. *J. Comp. Neurol.* **366**, 534–546.

Northcutt, R. G. (1989). The phylogenetic distribution and innervation of craniate mechanoreceptive lateral lines. In *The Mechanosensory Lateral Line. Neurobiology and Evolution* (ed. S. Coombs, P. Görner and H. Münz), pp 17–78. New York: Springer.

Oakley, B. and Schafer, R. (1978). *Experimental Neurobiology*. Ann Arbor: The University of Michigan Press.

Partridge, B. L. and Pitcher, T. J. (1980). The sensory basis of fish schools: relative roles of lateral line and vision. *J. Comp. Physiol. A* **135**, 315–325.

Pitcher, T. J. (1979). Sensory information and the organization of behavior in a shoaling fish. *Anim. Behav.* **27**, 126–149.

Pitcher, T. J., Partridge, B. L. and Wardle, C. S. (1976). A blind fish can school. *Science* **194**, 963–965.

Plachta, D., Mogdans, J. and Bleckmann, H. (1999). Responses of midbrain lateral line units of the goldfish, *Carassius auratus*, to constant-amplitude and amplitude-modulated water wave stimuli. *J. Comp. Physiol. A* **185**, 405–417.

Puzdrowski, R. L. (1989). Peripheral distribution and central projections of the lateral-line nerves in goldfish, *Carassius auratus*. *Brain Behav. Evol.* **34**, 110–131.

Satou, M., Shiraishi, A., Matsushima, T. and Okumoto, N. (1991a). Vibrational communication during spawning behavior in the hime salmon (landlocked red salmon, *Oncorhynchus nerka*). *J. Comp. Physiol. A* **168**, 417–428.

Satou, M., Takeuchi, H.-A., Nishii, J., Tanabe, M., Kitamura, S., Kudo, Y. and Okumoto, N. (1991b). Inter-sexual vibrational communication during spawning ehaviour in the hime salmon (landlocked red salmon, *Oncorhynchus nerka*). *Proc. Fourth Int. Symp. Reprod. Physiol. Fish* **1**, 185–187.

Song, J. and Northcutt, R. G. (1991). Morphology, distribution and innervation of the lateral-line receptors of the Florida gar, *Lepisosteus platyrhincus*. *Brain Behav. Evol.* **37**, 10–37.

Voigt, R., Carton, A. G. and Montgomery, J. C. (2000). Response of anterior lateral line afferent neurones to water flow. *J. Exp. Biol.* **203**, 2495–2502.

von Campenhausen, C., Riess, I. and Weissert, R. (1981). Detection of stationary objects in the blind cave fish *Anoptichthys jordani* (Characidae). *J. Comp. Physiol. A* **143**, 369–374.

Webb, J. F. (1989). Developmental constraints and evolution of the lateral line system in teleost fishes. In *The Mechanosensory Lateral Line. Neurobiology and Evolution* (ed. S. Coombs, P. Görner and H. Münz), pp. 79–98. New York: Springer.

Weissert, R. and von Campenhausen, C. (1981). Discrimination between stationary objects by the blind cave fish *Anoptichthys jordani*. *J. Comp. Physiol. A* **143**, 375–382.

Wojtenek, W., Mogdans, J. and Bleckmann, H. (1998). The responses of midbrain lateral line units of the goldfish, *Carassius auratus*, to objects moving in the water. *Zoology* **101**, 69–82.

Wubbels, R. J. (1992). Afferent response of a head canal neuromast of the ruff (*Acerina cernua*) lateral line. *Comp. Biochem. Physiol. A* **102A**, 19–26.